Article

A Highly Efficient Aggregation-induced Emission Photosensitizer for Photodynamic Combat of Multidrug-resistant Bacteria

ZOU Qian[1], WANG Jia-Li[1], WU Ming-Yu[1,2]✉, KAM Chuen[2], LEE Sin-Ying[2], FENG Shun[1] and CHEN Sijie[2]✉

Received November 27, 2020
Accepted December 24, 2020

With the antibiotic abuse and the resulting increased antibiotic resistance, the bacterial infection has posed a serious threat to human health. Photodynamic therapy is an effective tool for treating localized and superficial infections. It is a promising approach for the treatment of superbugs and with minimal risk of induced antibiotic resistance. Herein, an isoquinolinium-based photosensitizer, LIQ-TPE, with aggregation-induced emission properties is designed and synthesized. It is with high $^1O_2$ generation efficiency and shows efficient antibacterial performance towards both Gram-negative and Gram-positive bacteria, and even methicillin-resistant *Staphylococcus aureus*(MRSA). LIQ-TPE thus shows great promise as an effective antimicrobial agent to combat the menace of multi-drug resistant bacteria.

Keywords Aggregation-induced emission; Photosensitizer; Isoquinolinium; Photodynamic antibiosis

1 Introduction

Pathogenic bacteria have become a serious threat to global health, which cause various infections, resulting in severe illnesses and numerous outbreaks of food poisoning worldwide[1,2]. Antibiotic abuse and the resulting resistance to antibiotics heavily aggravate this threat[3,4]. Great efforts have been endeavored to search for new antibacterial agents. Nevertheless, the development of a new treatment is still far behind the spread of antibiotic-resistant bacteria[5]. The development of highly efficient antibacterial methods especially for multi-drug resistant bacteria is still of the utmost urgency but challenging.

As a prominent therapeutic strategy for contemporary and cost-effective precision medicine, photodynamic therapy (PDT) has attracted more and more attention in antibiosis[6]. It utilizes photosensitizers(PSs) and light illumination to generate cytotoxic reactive oxygen species(ROS), which cause oxidative damages to membrane lipids, nucleic acids, or proteins. Consequently, it induces irreversible bacterial cell death with the superiority in minimal invasiveness, limited antibiotic resistance, low systemic toxicity, and minimal side effects[7]. Despite a lot of conventional PSs, such as phenothiazinium salts, porphyrins, phthalocyanines, diketopyrrolopyrroles and cyanines, have been developed for photodynamic antibacterial purposes, and the bacteria-killing efficacy is unsatisfactory ascribing to the inherent drawback of aggregation-caused quenching(ACQ), resulting in nonradia-tive decay and low $^1O_2$ generation efficiency[8−10].

To address this issue, PSs with aggregation-induced emission(AIE) properties shed light on PDT[11−14]. The AIE luminophore shows weak or undetectable emission in dilute solution but emits strong fluorescence in the aggregated or solid state. This reduces nonradiative decay and increases $^1O_2$ production in the aggregate state as compared to that in the discrete molecular state[15]. As a result, several AIE-based PSs have been successfully developed as photodynamic antibiosis[16−23]. However, $^1O_2$ generation efficiency is still far from satisfactory. Developing new AIE PSs with high $^1O_2$ generation efficiency for antibacterial PDT is still challenging.

In our previous research[24,25], a simple Rh-catalyzed [4+2] annulation reaction was utilized to synthesize isoquinolinium-based AIE probes for chromosome periphery imaging or mitochondria imaging. After studying the relationship between structural differences and functional performances, it was found that the isoquinolinium salt showed ROS generation ability under white light illumination[26]. To improve the $^1O_2$ production and develop a more efficient PS, we further modified the probe by introducing a typical AIE group tetraphenyl ethylene(TPE) to synthesize LIQ-TPE. It showed higher $^1O_2$ generation efficiency than the widely used PS Rose Bengal(RB). It not only can be used for labelling and imaging Gram-positive or Gram-negative bacteria, but also works as an efficient photodynamic germicide for bacteria including multi-drug resistant bacteria.

✉ WU Ming-Yu
wumy1050hx@swjtu.edu.cn
✉ CHEN Sijie
sijie.chen@ki.se
1. School of Life Science and Engineering, Southwest Jiaotong University, Chengdu 610031, P. R. China;
2. Ming Wai Lau Centre for Reparative Medicine, Karolinska Institutet, Hong Kong, P. R. China

https://doi.org/10.1007/s40242-021-0393-2

2 Experimental

2.1 Materials and General Instruments

All chemical reagents were obtained from J&K Scientific and were used without further purification. 9,10-Anthracenediyl bis-(methylene)-dimalonic acid(ABDA) and Rose Bengal(RB) were purchased from Sigma-Aldrich. Thin-layer chromatography analyses were performed on a silica gel GF 254. Column chromatography purification was carried out on silica gel(200—300 mesh). NMR spectra were recorded using a Bruker AMX-400. Chemical shifts were given in δ relative to the internal reference TMS or $CDCl_3$ as the internal standard. High resolution mass spectra were recorded on a Bruker Daltonics Bio TOF mass spectrometer. Fluorescence spectra were obtained using a Horiba Duetta spectrofluorimeter with a 10 mm quartz cuvette. UV-Vis absorption spectra were recorded on a Hitachi PharmaSpec UV-1900 UV-Visible spectrophotometer. Confocal fluorescence images were recorded using a Zeiss LSM 880 confocal laser scanning microscope. The light source was a white LED illuminant from Opple Lighting Co., Ltd. with a power of 5 W, a diameter of 5 cm and an intensity of 20 mW/cm^2.

2.2 Synthesis and Characterization of LIQ-TPE

DMPEA-TPE: to a solution of TPE-COOH(376.5 mg, 1.0 mmol) in 20 mL of anhydrous DMF were added diisopropylamine (DIPEA, 646 mg, 5.0 mmol), DMPEA(235.6 mg, 1.3 mmol) and TBTU(455.2 mg, 1.2 mmol) successively under N_2. The mixture was then stirred at room temperature under N_2 overnight. Then, the solvent was evaporated under reduced pressure, the crude product was purified by silica gel flash column chromatography eluting with dichloromethane:ethyl acetate(10:1, volume ratio), affording DMPEA-TPE as a white solid of 496.5 mg(yield 92%).

IQ-TPE: to a solution of DMPEA-TPE(356.2 mg, 0.66 mmol) in PhMe(14 mL) was added a $POCl_3$(122.7 μL) solution in 1 mL of PhMe dropwisely under argon at room temperature. The reaction mixture was heated under reflux for 4—5 h. After being concentrated to dryness, the crude product was neutralized with 2 mol/L NaOH solution, extracted with 50 mL of CH_2Cl_2 thrice and washed with a saturated NaCl solution. The organic layers were dried with Na_2SO_4. The solvent was evaporated under reduced pressure, and the crude product was recrystallized with a mixed solution of dichloromethane: ethyl acetate(1:1, volume ratio) to give a yellow product of 318.7 mg(yield: 92.6%). ^{1}H NMR(400 MHz, $CDCl_3$), δ: 7.54(d, 2H, J=8.4 Hz), 7.24(d, 2H, J=8.4 Hz), 7.14—7.03(m, 15H), 6.86(s, 1H), 6.78(s, 1H), 4.00(s, 3H), 3.97(t, 2H, J=7.6 Hz), 3.72(s, 3H), 2.97(t, 2H, J=7.6 Hz). ^{13}C NMR(100 MHz, $CDCl_3$), δ: 147.9, 143.4, 143.1, 143.0, 142.5, 139.8, 134.4, 131.9, 131.5, 131.4, 131.2, 130.0, 128.0, 127.9, 127.8, 127.0, 126.9, 126.8, 114.2, 110.8, 56.5, 56.1, 53.4, 25.9. HRMS(ESI): m/z[M+H]$^+$ calcd. for $C_{37}H_{32}NO_2^+$: 522.2428; found: 522.2439.

LIQ-TPE: 260.8 mg of DMPEA-TPE(0.5 mmol), 89.1 mg of 1,2-diphenylethyne(0.5 mmol), 0.005 mmol of $[(Cp^*)RhCl_2]_2$ (3.1 mg), 165.7 mg of silver trifluoroacetate(0.75 mmol), and 90.8 mg of copper acetate(0.5 mmol) were added to 10 mL of ethyl alcohol. After heated to reflux with magnetic stirring for 30 min under N_2, the mixture was filtered through diatomite and washed with ethanol. The solvent was evaporated under reduced pressure, and the crude product was purified by column chromatography on silica gel[V(dichloromethane): V(MeOH)=20:1] to afford an orange product of 367.8 mg(yield 90.6%). ^{1}H NMR(400 MHz, $CDCl_3$), δ: 8.38(d, 1H, J=9.2 Hz), 7.51(dd, 1H, J=1.6 Hz, 8.8 Hz), 7.39(d, 1H, J=1.6 Hz), 7.36(s, 1H), 7.31(s, 5H), 7.21—7.08(m, 13H), 7.00—6.94(m, 6H), 6.69(d, 2H, J=8.8 Hz), 4.36(t, 2H, J=6.4 Hz), 4.04(s, 3H), 3.90(s, 3H), 3.21(t, 2H, J=6.4 Hz). ^{13}C NMR(100 MHz, $CDCl_3$), δ: 154.4, 152.8, 151.7, 148.2, 145.7, 144.2, 142.5, 142.4, 142.0, 138.6, 138.1, 135.4, 133.6, 133.5, 133.2, 131.6, 131.4, 131.2, 130.4, 130.3, 130.1, 129.7, 129.4, 129.0, 128.5, 128.3, 128.2, 128.0, 127.8, 127.5, 127.4, 127.3, 123.3, 118.8, 115.9, 110.9, 56.7, 56.6, 52.1, 27.2. HRMS(ESI): m/z[M–CF_3COO^-]$^+$ calcd. for $C_{51}H_{40}NO_2$: 698.3054; found: 698.3069.

2.3 $^1O_2$ Generation Efficiency Measurement

The $^1O_2$ generation was measured using ABDA as an indicator, and RB was employed as the standard photosensitizer. ABDA(50 μmol/L) was mixed with the LIQ-TPE or RB(5 μmol/L) in DMSO/water(volume ratio 1:99) and exposed to white light illumination(20 mW/cm^2). The absorbance of ABDA at 378 nm was recorded at different illumination time to obtain the decay rate of the photosensitizing process.

2.4 Bacteria Culture, Staining and Imaging

Enterococcus faecalis(*E. faecalis*), *Escherichia coli*(*E. coli*) and *Pseudomonas aeruginosa*(*P. aeruginosa*) were from China General Microbiological Culture Collection Center(CGMCC), while *Staphylococcus epidermidis*(*S. epidermidis*) was from American Type Culture Collection(ATCC). Methicillin-resistant *Staphylococcus aureus*(MRSA) was kindly provided by the Sichuan Industrial Institute of Antibiotics, Chengdu University, China. A single colony of bacteria on solid culture medium was transferred to 10 mL of the corresponding liquid culture medium[Lysogeny broth(LB) for *E. coli*, *P. aeruginosa* and MRSA; Tryptic Soy Agar(TSA) for *E. faecalis*; Nutrient Broth(NB) for *S. epidermidis*], and grown at 37 °C for 6—8 h with a shaking speed of 200 r/min. After being harvested by

https://doi.org/10.1007/s40242-021-0393-2

centrifuging at 8000 r/min for 5 min, the bacteria were washed with PBS three times and re-suspended with PBS, and diluted to an optical density(about 10^8 CFU/mL). The concentrations of the bacterial suspension were determined *via* optical density measurements of absorbance at 600 nm using a cell density meter.

Then, 500 μL of bacteria(about 10^8 CFU/mL) in a 1.5 mL centrifuge tube were harvested by centrifuging at 8000 r/min for 5 min. After removed the supernatant and washed with PBS, 1 μL of 2.5 mmol/L LIQ-TPE stock solution was added to the dispersed bacteria in 0.5 mL of PBS solution and incubated at 37 °C for 20 min. After harvested by centrifuging at 8000 r/min for 5 min, the bacteria were washed with PBS three times. About 2.5 μL of staining bacteria was transferred to a glass slide and then covered with a coverslip for imaging with a Zeiss LSM 880 laser scanning confocal microscope equipped with a Plan-Apochromat 63×/1.4 NA oil objective lens, a photo-multiplier tube, and a Gallium arsenide phosphide detector driven by the ZEN software(Carl Zeiss). The 405 nm laser and 550—650 nm emission filters were used for LIQ-TPE.

2.5 Photodynamic Antibiosis

First, 1 μL of LIQ-TPE stock solution(2 mmol/L) or PBS was added to 1 mL of prepared bacteria PBS solution(about 10^8 CFU/mL) in a 1.5 mL centrifuge tube(*E. coli*, *P. aeruginosa*, *E. faecalis*, *S. epidermidis* and MRSA) and incubated at 37 °C for 10 min under dark. After centrifuged the bacterial suspensions at 8000 r/min for 5 min, the supernatant was removed and washed with PBS three times. The bacteria were dispersed again in PBS and either exposed to white light(20 mW/cm^2) or incubated under dark for 30 min. Then, the bacteria were transferred onto an agar plate and incubated at 37 °C overnight. The bacteria viability was then determined and quantified by the plate count method.

2.6 Scanning Electron Microscopy(SEM) Analysis

After treated with the above mentioned photodynamic antibacterial experiments, bacteria were fixed with 2.5% glutaraldehyde PBS solution at 4 °C overnight and then centrifuged at 8000 r/min for 5 min. The supernatant was removed, and the bacteria were washed with sterile water three times, then dehydrated by different contents of ethanol(30%, 50%, 70%, 85%, and 95% for 5 min, respectively, and 100% for 15 min twice), and dried in a vacuum drying oven. The specimens were coated with platinum before SEM analysis(Phenom ProX Desktop SEM).

3 Results and Discussion

3.1 Synthesis and Optical Properties

The synthetic route to LIQ-TPE is illustrated in Scheme 1. First, the amide DMPEA-TPE was obtained through an amide condensation reaction between amine(DMPEA) and carboxylic acid(TPE-COOH) with the condensation agent of TBTU and DIPEA in a yield of 92%. Then, a highly efficient cyclodehydration reaction of amide for the synthesis of isoquinoline (IQ-TPE) under strong acid condition was performed with a yield of 92.6%. Finally, the aim product LIQ-TPE was synthesized through a $[RhCp^*Cl_2]_2$ catalyzed [4+2] annulation reaction with high yields of more than 90.6%. These products were characterized by ^{1}H NMR, ^{13}C NMR, and mass spectrometry(see the Electronic Supplementary Material of this paper).

The optical properties of LIQ-TPE are illustrated in Fig.1 and Fig.S1(see the Electronic Supplementary Material of this paper). By photoluminescence spectrometry, LIQ-TPE showed its maximum absorption peak at 415 and 580 nm with a large Stokes shift of 165 nm[Fig.1(A)]. To further investigate the AIE features of LIQ-TPE, a tetrahydrofuran/phosphate buffer solution(THF/PBS) mixed with different PBS fractions(volume ratio) was utilized as the solvent system. As depicted in Fig.1(B) and 1(C), LIQ-TPE showed low fluorescence emission in pure THF solution with the quantum yield(QY) of 2.98%. When adding PBS to the THF solution, the fluorescence slightly decreased at first along with the water fractions increased from 10% to 80%, and this result could be attributed to the twisted intramolecular charge transfer(TICT) effect. When the ratio of PBS in the mixed solvent was further increased from 90% to 99.9%, the fluorescence intensity of LIQ-TPE

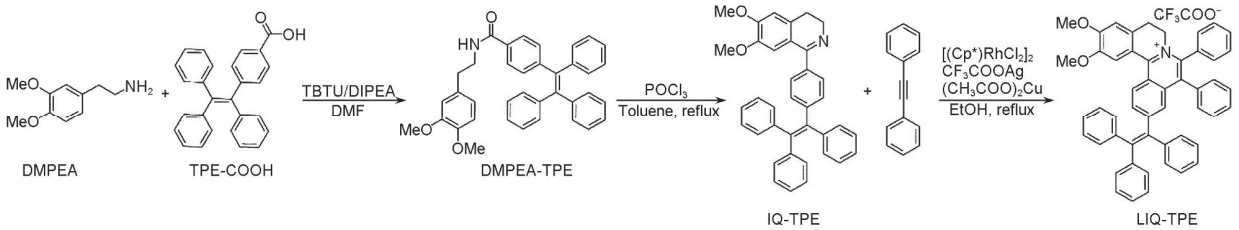

Scheme 1 Synthetic route of LIQ-TPE

https://doi.org/10.1007/s40242-021-0393-2

rebounded dramatically due to the formation of the probe aggregates(QY: 23.5%), and the fluorescence intensity of LIQ-TPE in 99% PBS solution was 5.03 folds of that in pure THF solution. The aggregate formed with an average size of approximately 252.5 nm in diameter was confirmed by dynamic light scattering[Fig.1(D)]. As a result, these data affirmatively revealed the AIE characteristics of LIQ-TPE.

3.2 $^1O_2$ Generation Efficiency Study

Subsequently, the $^1O_2$ generation ability of LIQ-TPE was studied by measuring changes in the absorption spectra of the $^1O_2$ indicator, ABDA[27], with white-light illumination(20 mW/cm^2). As illustrated in Fig.2, the absorbance of the

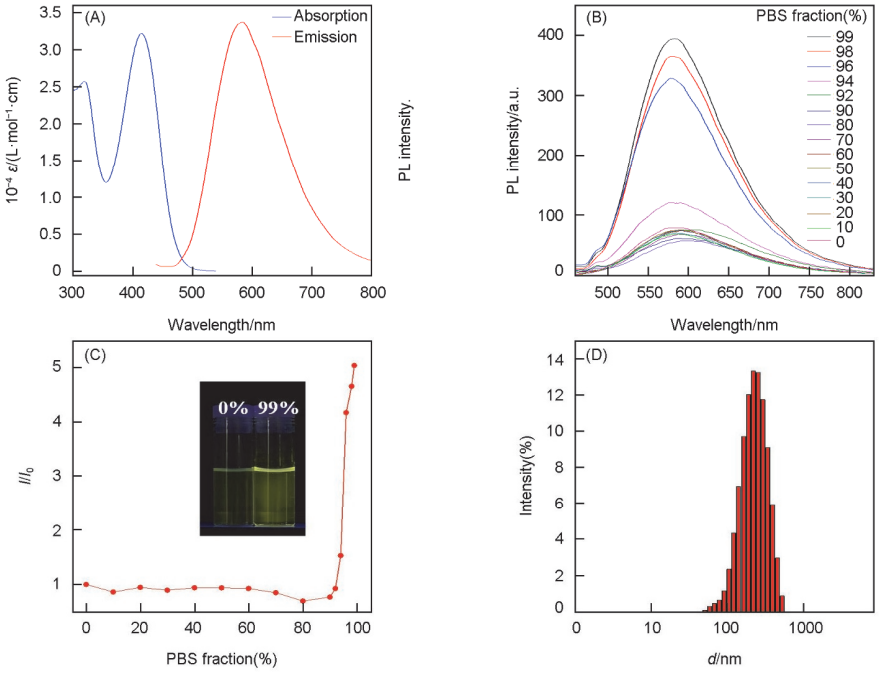

Fig.1 General optical properties of LIQ-TPE

(A) Molar absorption coefficient and emission spectra of LIQ-TPE; (B) PL spectra of LIQ-TPE(10 μmol/L) in mixtures of THF and PBS with different PBS contents; (C) plot of the relative emission intensity of LIQ-TPE *versus* PBS fraction, I_0 and I are the peak values of PL intensities of LIQ-TPE(10 μmol/L) in THF and THF/PBS mixtures, respectively. Inset: fluorescence images of LIQ-TPE in THF solution(left) and aggregated(99% PBS, right) with 365 nm excitation; (D) size distribution of LIQ-TPE in the mixture of THF/PBS with 99% water content.

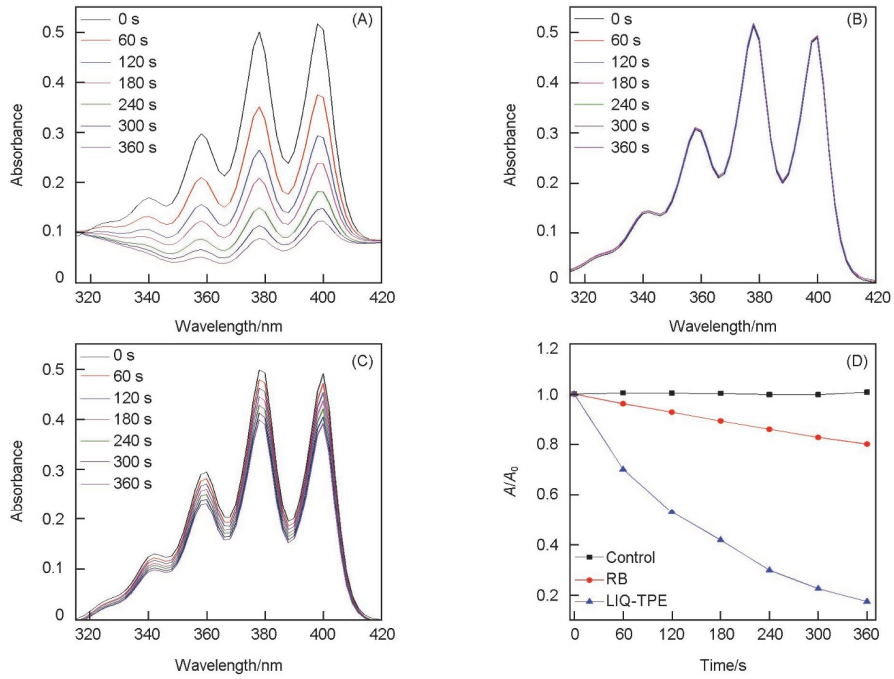

Fig.2 $^1O_2$ generation efficiency of LIQ-TPE

UV/Vis spectra of ABDA in the presence of LIQ-TPE(A), blank control(B) and RB(C) under white-light illumination; (D) decomposition rates of ABDA in the absence or presence of LIQ-TPE, and RB under light illumination, where A_0 and A are the initial and final, respectively, absorbances of ABDA at 378 nm.

https://doi.org/10.1007/s40242-021-0393-2

ABDA(50 mmol/L) at 378 nm in the solution containing LIQ-TPE(5 μmol/L) gradually decreased to 17.6% upon white light illumination from 0 to 6 min[Fig.2(A) and (D)]. However, the absorption profile of ABDA solution almost showed no change under the same condition without LIQ-TPE[Fig.2(B) and (D)]. These results clearly demonstrated that LIQ-TPE could efficiently generate $^1O_2$. Subsequently, the commercial PS, RB, was compared. Under the same condition, the absorbance of ABDA at 378 nm in solution containing 5 μmol/L RB decreased to 80%[Fig.2(C) and (D)]. LIQ-TPE is far superior to RB as a PS. The decomposition rate constants of ABDA by LIQ-TPE are 4.5 folds of that of RB(Fig.S2, see the Electronic Supplementary Material of this paper).

3.3 Photodynamic Antibacterial Activity

To determine whether LIQ-TPE could target bacteria, LIQ-TPE staining on different types of bacteria was performed. As shown in Fig.3, both Gram-positive bacteria(*S. epidermidis*) and Gram-negative bacteria(*E. coli*) could be fluorescently labelled after 20 min of incubation with 2.5 μmol/L LIQ-TPE, suggesting that LIQ-TPE could successfully label both Gram-positive and Gram-negative bacteria.

Inspired by the remarkable performance in the AIE feature and high $^1O_2$ generation efficiency, we further explored LIQ-TPE for photodynamic antibacterial effect through the plate-counting method. Taking *E. faecalis* as an example, the dose-dependent photodynamic antibacterial study was first performed upon different concentrations of LIQ-TPE(0, 0.5, 1.0, and 2.0 μmol/L) treatment with or without light illumination (20 mW/cm^2). As shown in Fig.S3(see the Electronic Supplementary Material of this paper), LIQ-TPE exerted negligible toxicity to *E. faecalis* without light illumination process in all tested concentrations. After 30 min of white light illumination, the viability of LIQ-TPE-treated *E. faecalis* rapidly decreased. As shown in Fig.S3, most bacteria were eliminated after being treated with 0.5 μmol/L of LIQ-TPE and light illumination. Once the concentration exceeded 1 μmol/L, hardly any bacterial colonies grew on the plate were observed. Subsequently, the antibacterial PDT performance of LIQ-TPE at 2.0 μmol/L was tested against the growth of different kinds of Gram-positive(*E. faecalis* and *S. epidermidis*) and Gram-negative(*E. coli* and *P. aeruginosa*) bacteria. As shown in Fig.4, both *E. faecalis* and *S. epidermidis* grew normally in PBS. Exposing the bacteria to white light illumination did not have any adverse effect on their growth rates. Meanwhile, the numbers of colonies did not change much when the bacteria were treated with 2.0 μmol/L LIQ-TPE and cultured in the dark. However, further exposing the bacteria to white light illumination for another 30 min prior to spread-plating significantly inhibited the bacterial growth on the plate. Gram-negative bacteria have a complex membrane structure which acts as a unique permeability barrier to protect the bacteria from antibiotics[28]. Nevertheless, LIQ-TPE showed the same performance in photodynamic ablation of Gram-negative bacterial growth exemplified by both *E. coli* and *P. aeruginosa*. After being treated with 2.0 μmol/L LIQ-TPE for 10 min followed by white light illumination, *E. coli* and *P. aeruginosa* were unable to grow into bacterial colonies. It is known that MRSA is a type of dangerous drug-resistant bacteria, which is commonly associated with several difficult-to-treat infections in humans and results in a global threat[29]. From our data, LIQ-TPE could efficiently kill MRSA through PDT. More than 99.9% of MRSA were killed upon 2 μmol/L LIQ-TPE treatment under light illumination compared with the PBS group(Fig.4). As a control, no significant inhibition was found in the groups treated with LIQ-TPE or white light illumination alone.

Moreover, scanning electron microscopy(SEM) was employed to visualize the morphological changes of the bacteria(Fig.5). Both *S. epidermidis* and *P. aeruginosa* in PBS

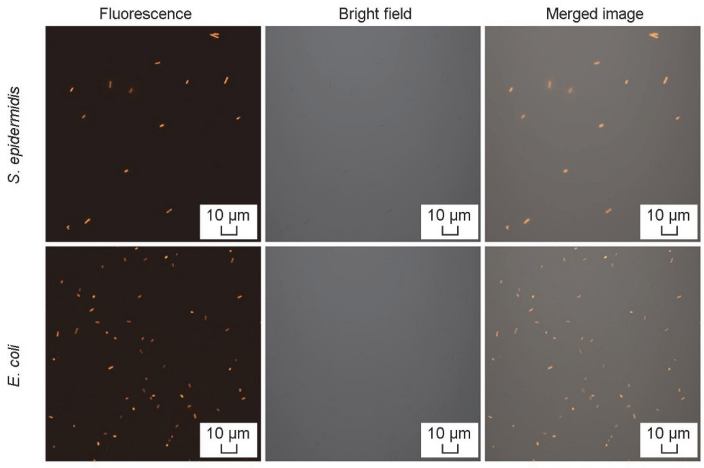

Fig.3 Fluorescence imaging of Gram-positive bacteria(*S. epidermidis*) and Gram-negative bacteria(*E. coli*) stained with 2.5 μmol/L LIQ-TPE

https://doi.org/10.1007/s40242-021-0393-2

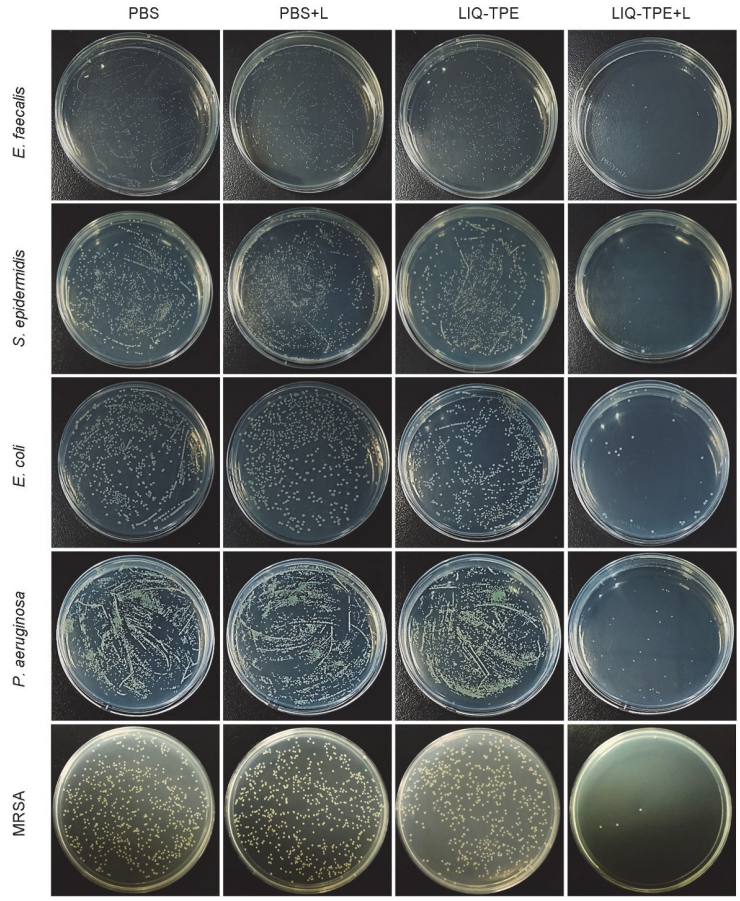

Fig.4 Plates images of *E. faecalis*, *S. epidermidis*, *E. coli*, *P. aeruginosa* and MRSA after treatment with PBS or LIQ-TPE(2 μmol/L) for 10 min without or with light illumination(20 mW/cm^2) for 30 min

L: white light illumination.

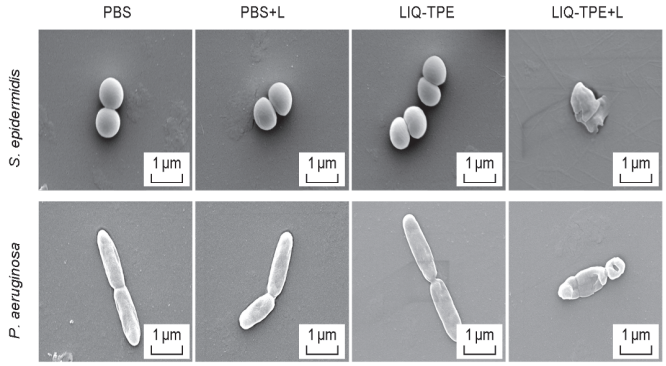

Fig.5 SEM images of *S. epidermidis* and *P. aeruginosa* after treatment with PBS or LIQ-TPE(2 μmol/L) in the absence or presence of white light illumination for morphological analysis

L: white light illumination.

showed well-defined and clear membrane boundaries with smooth surfaces. Their morphologies show no observable difference under white light illumination or in LIQ-TPE treatment. In contrast, ruptured bacteria with rough and irregular cell walls could be observed after LIQ-TPE treatment with white light illumination, which unambiguously confirmed that both LIQ-TPE and light illumination were necessary conditions for powerful elimination of bacteria. These results demonstrated the capability and efficiency of LIQ-TPE in killing both Gram-positive and Gram-negative bacteria.

4 Conclusions

In summary, an AIE active isoquinolinium-based PS, LIQ-TPE, was developed. It had high $^1O_2$ generation efficiency, which is

https://doi.org/10.1007/s40242-021-0393-2

far superior to the most popularly used PS, RB. LIQ-TPE can effectively label both Gram-positive and Gram-negative bacteria. It also showed good performance in the photodynamic ablation of common bacteria as well as multidrug-resistant bacteria, MRSA. This work provides a valuable tool for photodynamic antibacterial applications.

Electronic Supplementary Material

Supplementary material is available in the online version of this article at http://dx.doi.org/10.1007/s40242-021-0393-2.

Acknowledgements

This work was supported by the National Natural Science Foundation of China(No.21708030) and the Start-up Funding from Ming Wai Lau Centre for Reparative Medicine, Karolinska Institutet.

Availability of Data and Materials

All data generated or analyzed during this study are included in this published article and its supplementary information files.

Conflicts of Interest

The authors declare no conflicts of interest.

References

[1] Heymann D. L., *Cell*, **2006**, *124*, 671
[2] Reinhart K., Daniels R., Kissoon N., Machado F. R., Schachter R. D., Finfer S., *N. Engl. J. Med.*, **2017**, *377*, 414
[3] Chait R., Craney A., Kishony R., *Nature*, **2007**, *446*, 668
[4] Blair J. M., Webber M. A., Baylay A. J., Ogbolu D. O., Piddock L. J., *Nat. Rev. Microbiol.*, **2015**, *13*, 42
[5] Brown E. D., Wright G. D., *Nature*, **2016**, *529*, 336
[6] Dolmans D. E., Fukumura D., Jain R. K., *Nat. Rev. Cancer*, **2003**, *3*, 380
[7] Lucky S. S., Soo K. C., Zhang Y., *Chem. Rev.*, **2015**, *115*, 1990
[8] Cieplik F., Deng D., Crielaard W., Buchalla W., Hellwig E., Ahmad A., Maisch T., *Crit. Rev. Microbiol.*, **2018**, *44*, 571
[9] Kamkaew A., Lim S. H., Lee H. B., Kiew L. V., Chung L. Y., Burgess K., *Chem. Soc. Rev.*, **2013**, *42*, 77
[10] Hu F., Xu S., Liu B., *Adv. Mater.*, **2018**, *30*, 1801350
[11] Mei J., Leung N. L., Kwok R. T., Lam J. W., Tang B. Z., *Chem. Rev.*, **2015**, *115*, 11718
[12] Wu W., Mao D., Xu S., Ji S., Hu F., Ding D., Kong D., Liu B., *Mater. Horiz.*, **2017**, *4*, 1110
[13] Zhu C., Kwok R. T. K., Lam J. W. Y., Tang B. Z., *ACS Appl. Bio Mater.*, **2018**, *1*, 1768
[14] Zhao Z., Zhang H., Lam J. W. Y., Tang B. Z., *Angew. Chem. Int. Ed.*, **2020**, *59*, 9888
[15] Wang D., Lee M. M. S., Xu W., Kwok R. T. K., Lam J. W. Y., Tang B. Z., *Theranostics*, **2018**, *8*, 4925
[16] He X., Xiong L. H., Zhao Z., Wang Z., Luo L., Lam J. W. Y., Kwok R. T. K., Tang B. Z., *Theranostics*, **2019**, *9*, 3223
[17] Zhao E., Chen Y., Wang H., Chen S., Lam J. W. Y., Leung C. W. T., Hong Y., Tang B. Z., *ACS Appl. Mater. Interfaces*, **2015**, *7*, 7180
[18] Chen H., Li S., Wu M., Kenry, Huang Z., Lee C. S., Liu B., *Angew. Chem. Int. Ed.*, **2020**, *59*, 632
[19] Lee M. M. S., Xu W., Zheng L., Yu B., Leung A. C. S., Kwok R. T. K., Lam J. W. Y., Xu F.-J., Wang D., Tang B. Z., *Biomaterials*, **2020**, *230*, 119582
[20] Mao D., Hu F., Kenry., Qi G., Ji S., Wu W., Kong D., Liu B., *Mater. Horiz.*, **2020**, *7*, 1138
[21] Gao S., Yan X., Xie G., Zhu M., Ju X., Stang P. J., Tian Y., Xiu Z., *Proc. Natl. Acad. Sci. USA*, **2019**, *116*, 23437
[22] Shi X., Sung S. H. P., Chau J. H. C., Li Y., Liu Z., Kwok R. T. K., Liu J., Xiao P., Zhang J., Liu B., Lam J. W. Y., Tang B. Z., *Small Methods*, **2020**, 2000046
[23] Li Y., Zhao Z., Zhang J., Kwok, R. T. K., Xie S., Tang R., Jia Y., Yang J., Lam J. W. Y., Zheng W. F., Jiang X., Tang B. Z., *Adv. Funct. Mater.*, **2018**, *28*, 1804632
[24] Liu L., Zou Q., Leung J.-K., Wang J.-L., Kam C., Chen S., Feng S., Wu M.-Y., *Chem. Commun.*, **2019**, *55*, 14681
[25] Wu M.-Y., Leung J.-K., Liu L., Kam C., Chan K. Y. K., Li R. A., Feng S., Chen S., *Angew. Chem., Int. Ed.*, **2020**, *59*, 10327
[26] Wu M.-Y., Liu L., Zou Q., Leung J.-K., Wang J.-L., Chou T. Y., Feng S., *J. Mater. Chem. B*, **2020**, *8*, 9035
[27] Lindig B. A., Rodgers M. A., Schaap A. P., *J. Am. Chem. Soc.*, **1980**, *102*, 5590
[28] Henderson J. C., Zimmerman S. M., Crofts A. A., Boll J. M., Kuhns L. G., Herrera C. M., Trent M. S., *Annu. Rev. Microbiol.*, **2016**, *70*, 255
[29] Blair J. M., Webber M. A., Baylay A. J., Ogbolu D. O., Piddock L. J., *Nat. Rev. Microbiol.*, **2015**, *13*, 42